Electronic Supplementary Material (ESI) for Dalton Transactions.

Efficient yellow electroluminescence of four iridium(III) complexes with benzo[*d*]thiazole derivatives as main ligands

Zhi-Gang Niu[1,2], Jun Chen[1], Peng Tan[2], Wei Sun[2], You-Xuan Zheng[*,1], Gao-Nan Li[*,2], Jing-lin Zuo[*,1]

[1] *State Key Laboratory of Coordination Chemistry, Jiangsu Key Laboratory of Advanced Organic Materials, Collaborative Innovation Center of Advanced Microstructures, School of Chemistry and Chemical Engineering, Nanjing University, Nanjing 210093, P. R. China, yxzheng@nju.edu.cn zuojl@nju.edu.cn*

2 College of Chemistry and Chemical Engineering, Hainan Normal University, Haikou 571158, P. R. China, ligaonan2008@126.com

1. General information

X-ray diffraction data were collected with an Agilent Technologies Gemini A Ultra diffractometer equipped with graphite-monochromatedMo Kα radiation (λ = 0.7107 Å) at room temperature. Data collection and reduction were processed with CrysAlisProsoftware.[1] All of the structures were solved using Superflip[20] and refined using SHELXL–2014[2] within Olex2.[3] All calculations were carried out with Gaussian 09 software package.[4] The density functional theory (DFT) and time-dependent DFT (TDDFT) were employed with no symmetry constraints to investigate the optimized geometries and electron configurations with the Becke three-parameter Lee-Yang-Parr (B3LYP) hybrid density functional theory.[5–8]

2. OLED fabrication and measurement

All OLEDs were fabricated on the pre-patterned ITO-coated glass substrate with a sheet resistance of 10 $\Omega\cdot sq^{-1}$. The deposition rate for organic compounds is 1-2 $Å\cdot s^{-1}$. The phosphor and the host TCTA or 2,6DCzPPy were co-evaporated to form emitting layer from two separate sources. The cathode consisting of LiF/Al was deposited by evaporation of LiF with a deposition rate of 0.1 $Å\cdot s^{-1}$ and then by evaporation of Al metal with a rate of 3 $Å\cdot s^{-1}$. The characteristic curves of the devices were measured with a computer which controlled KEITHLEY 2400 source meter with a calibrated silicon diode in air without device encapsulation. On the basis of the uncorrected PL and EL spectra, the Commission Internationale de l'Eclairage (CIE) coordinates were calculated using a test program of the Spectra scan PR650 spectrophotometer.

3. NMR and MS characterization of ligands and complexes.

¹H NMR of 6-fluoro-2-phenylbenzo[d]thiazole (3b)

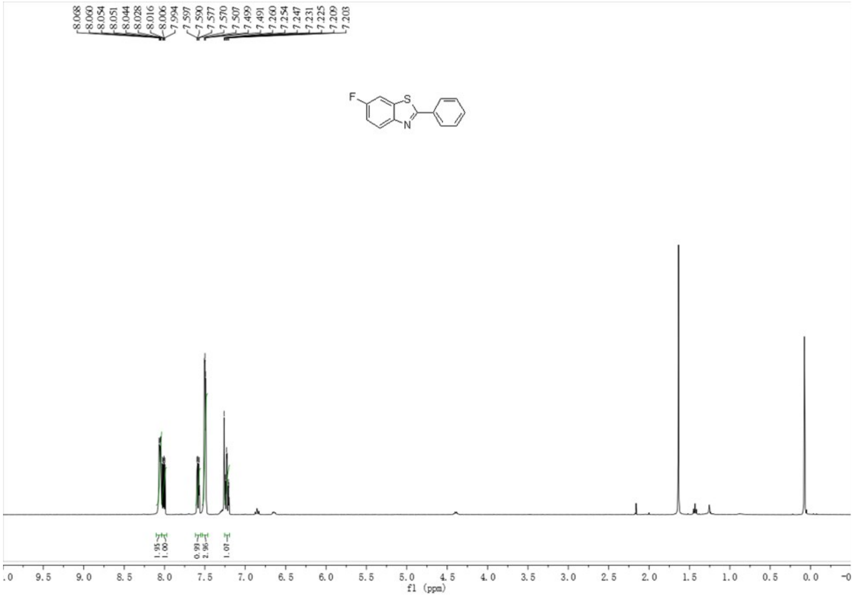

¹H NMR of 2-phenyl-6-(trifluoromethyl)benzo[d]thiazole (3c)

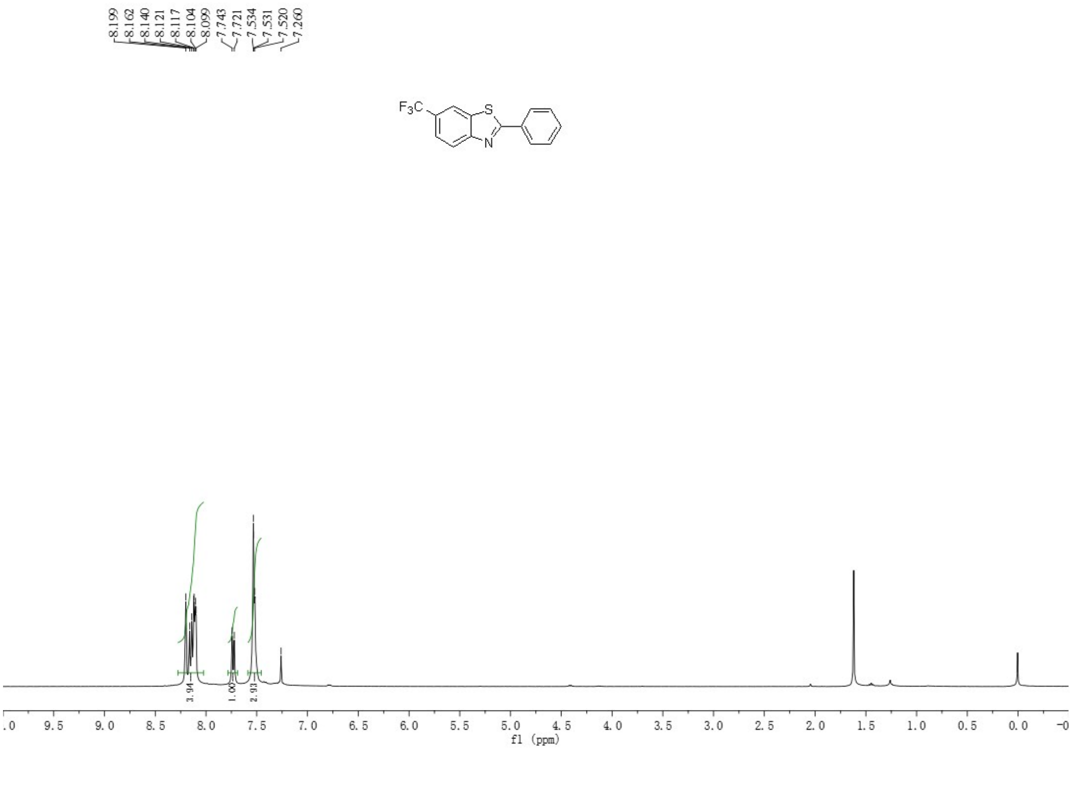

^{1}H NMR of 5,7-Difluoro-2-phenylbenzo[d]thiazole (3d)

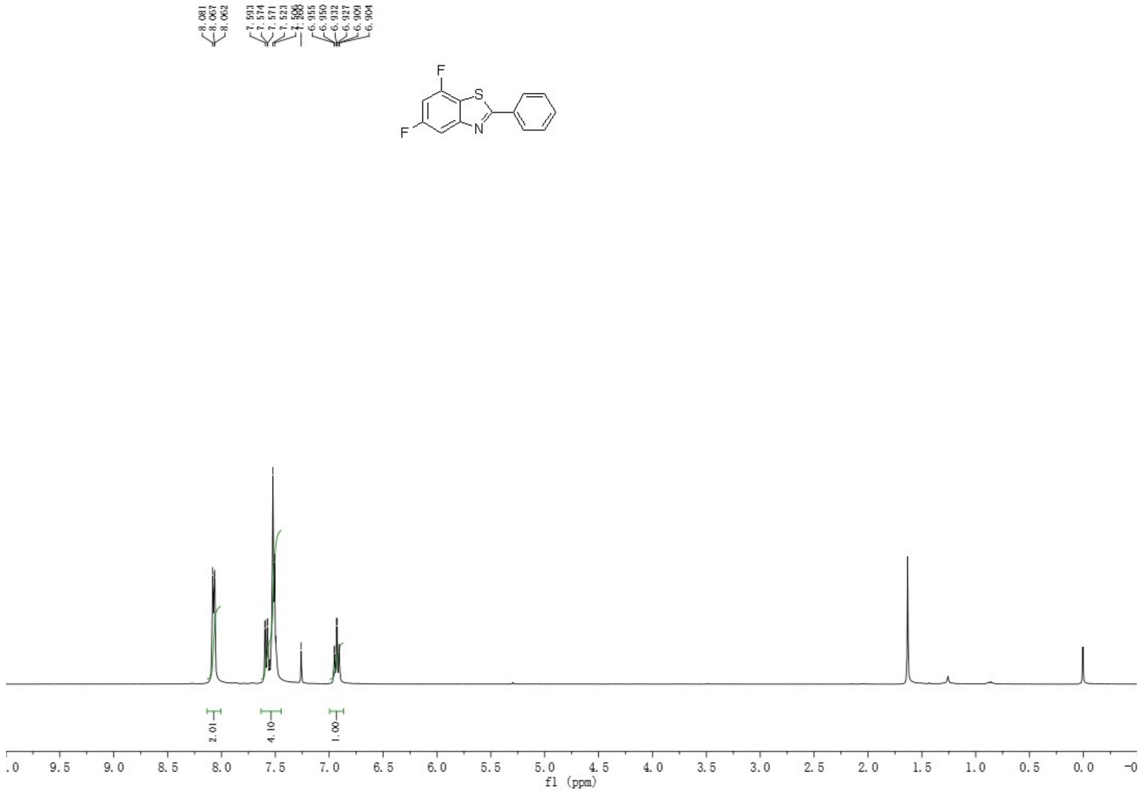

MS of $(bt)_2Ir(tpip)$

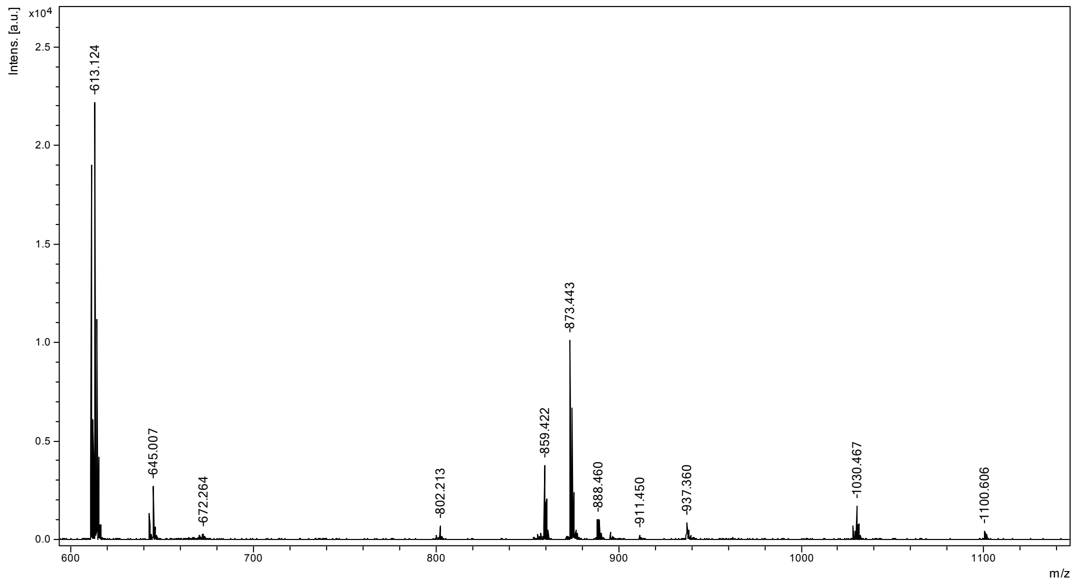

^{1}H **NMR of (bt)$_2$Ir(tpip)**

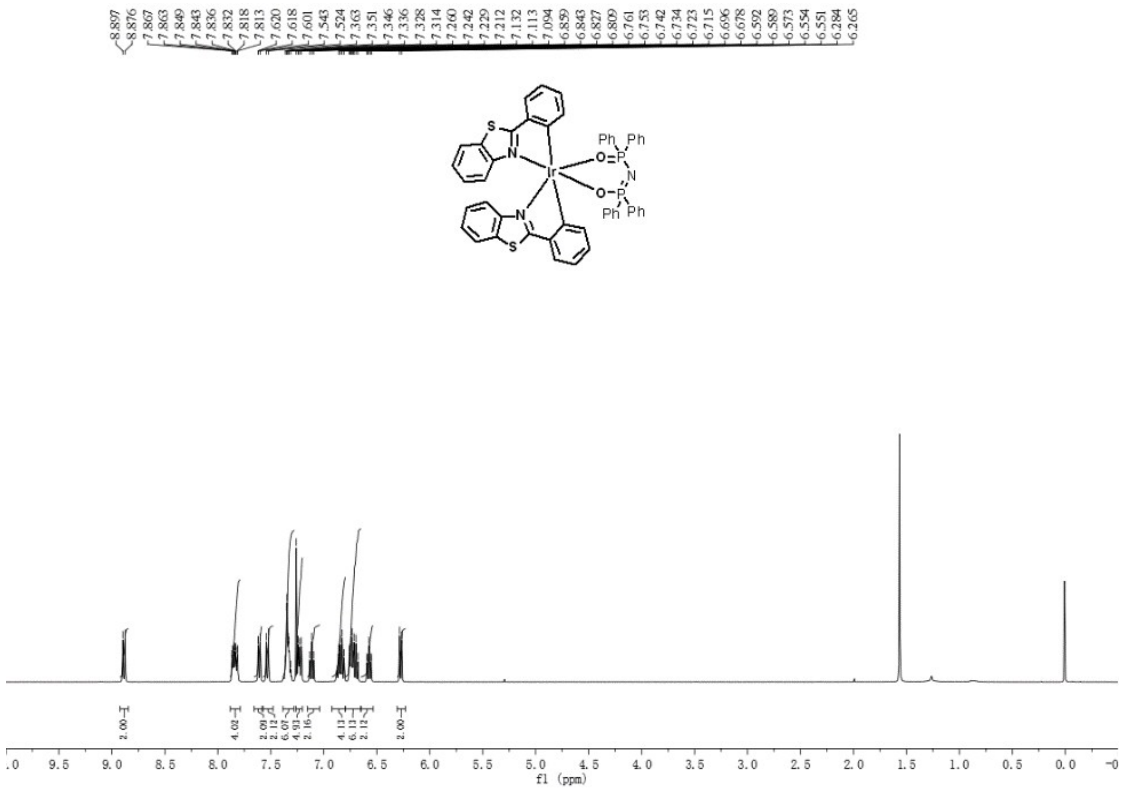

^{31}P **NMR of (bt)$_2$Ir(tpip)**

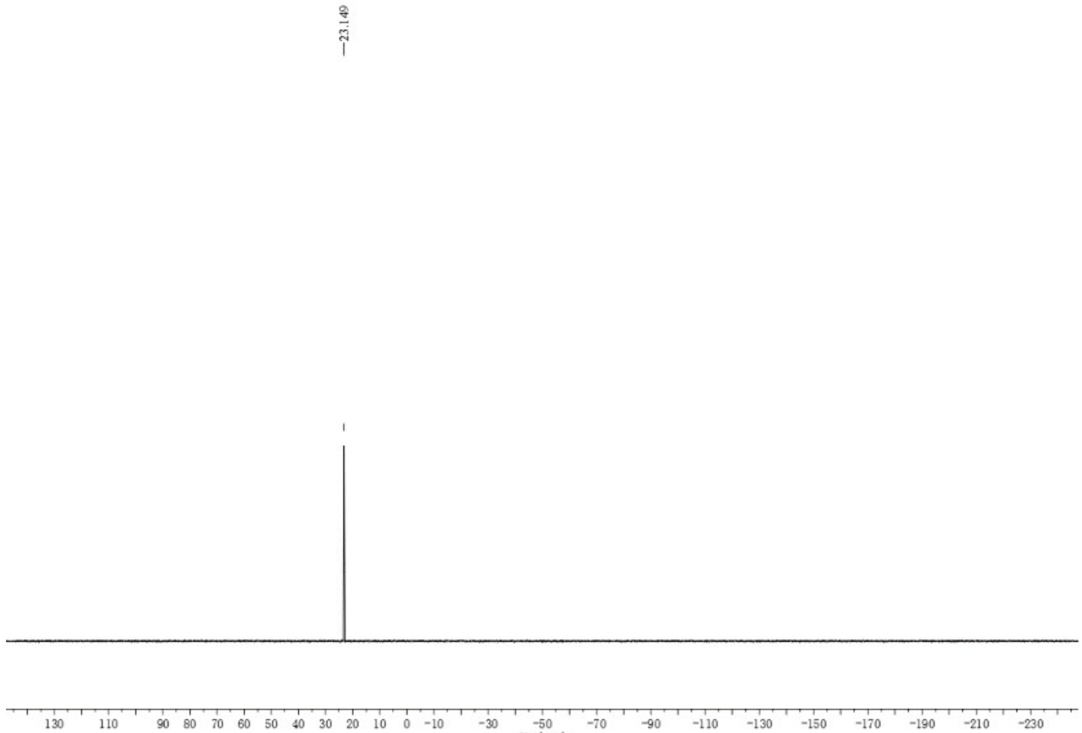

MS of (fbt)$_2$Ir(tpip)

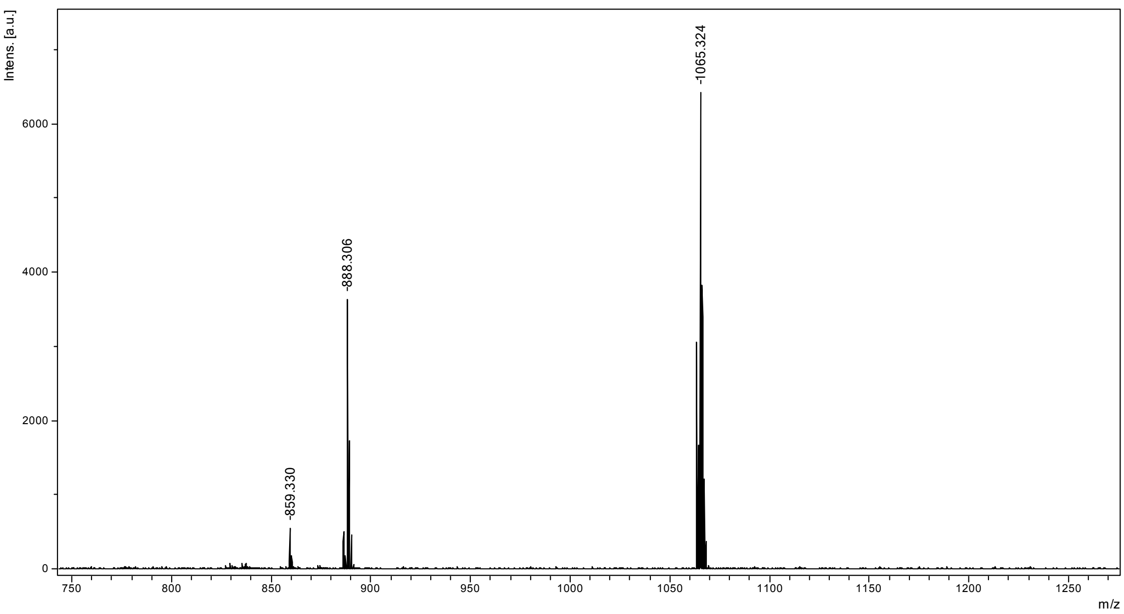

[1]H NMR of (fbt)$_2$Ir(tpip)

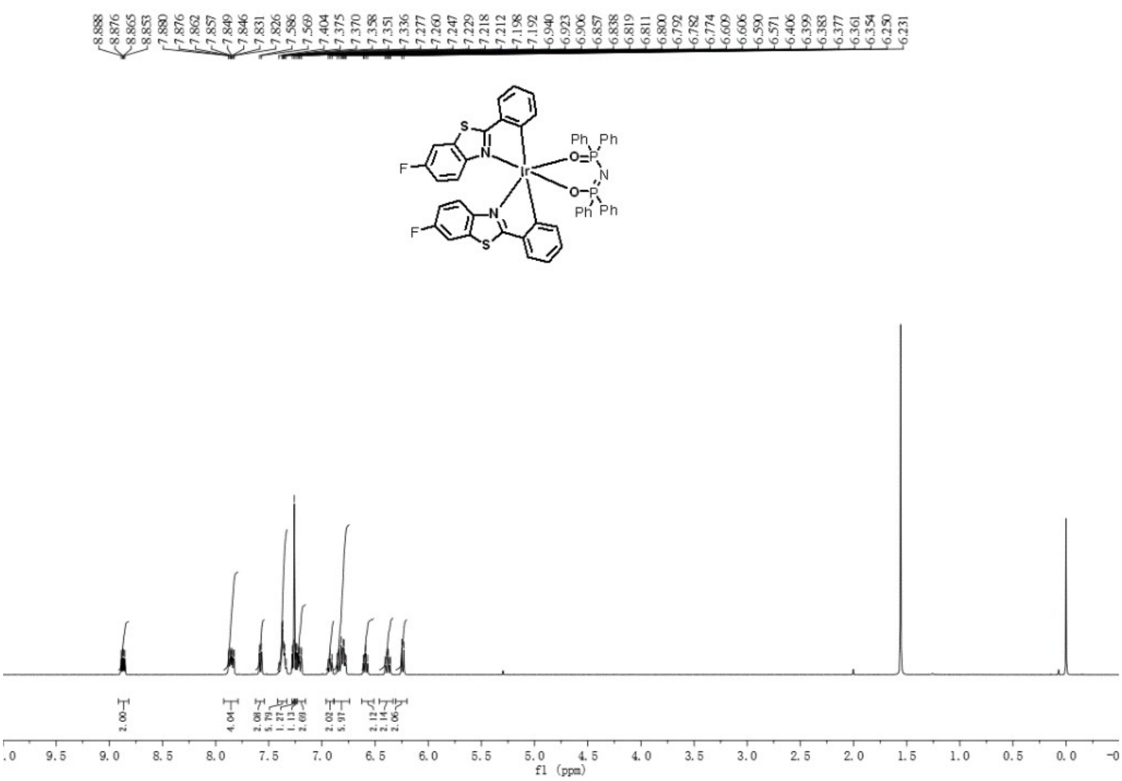

^{19}F NMR of $(fbt)_2Ir(tpip)$

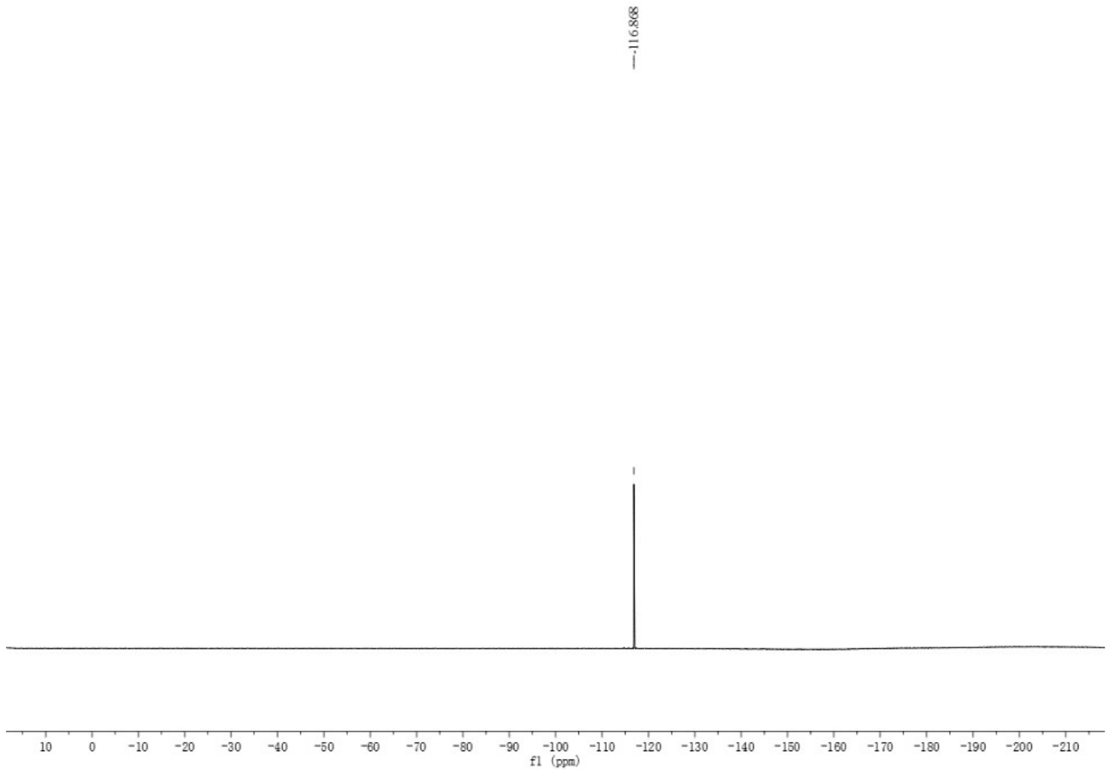

^{31}P NMR of $(fbt)_2Ir(tpip)$

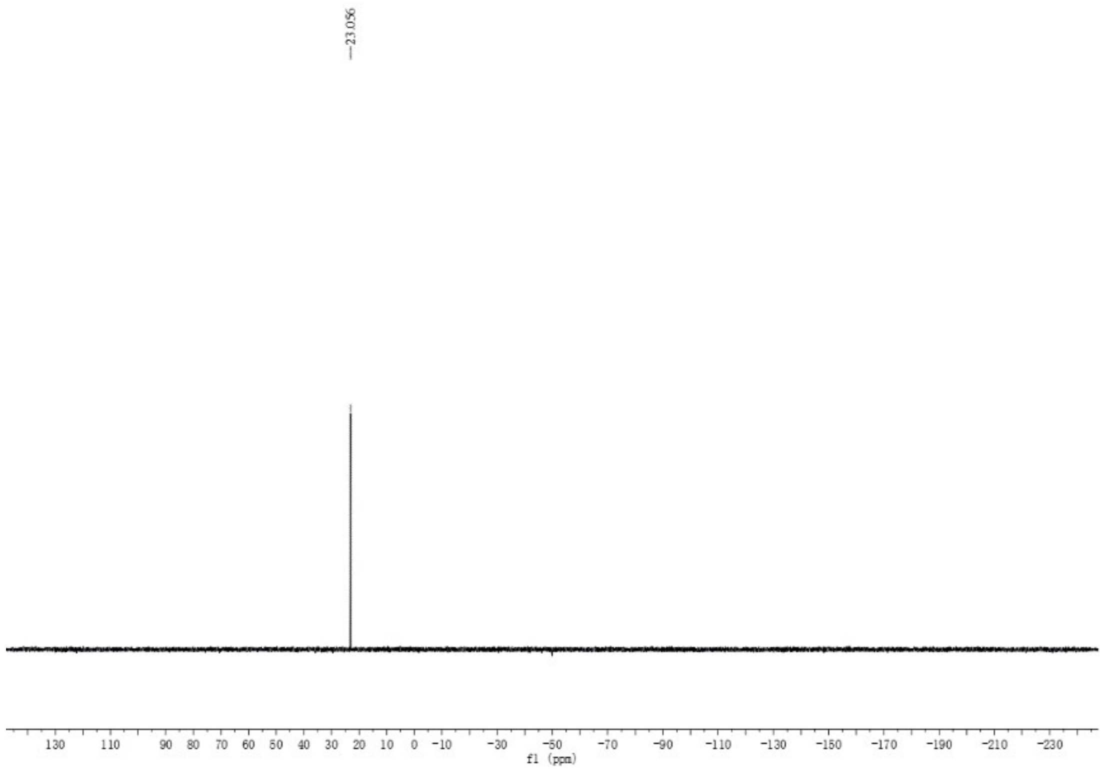

MS of $(cf_3bt)_2Ir(tpip)$

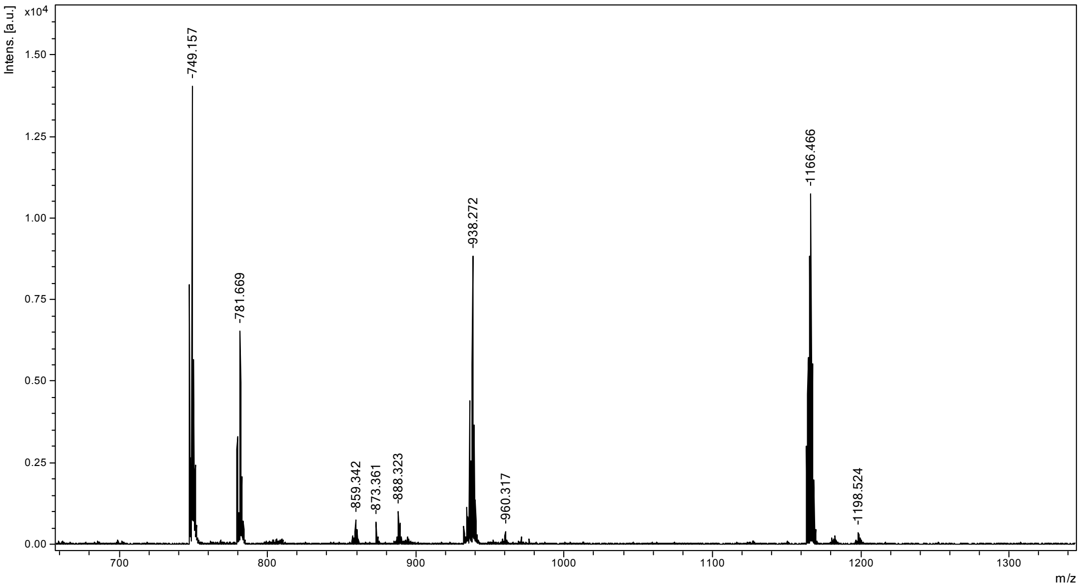

^1H NMR of $(cf_3bt)_2Ir(tpip)$

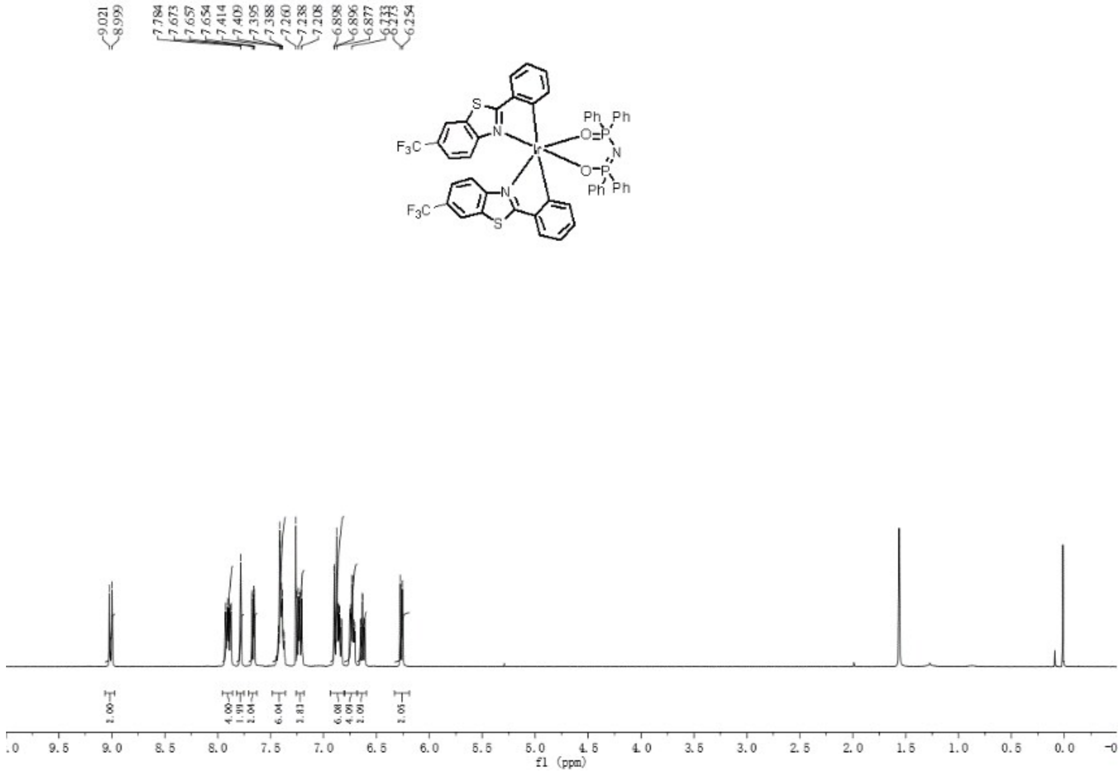

^{19}F NMR of $(cf_3bt)_2Ir(tpip)$

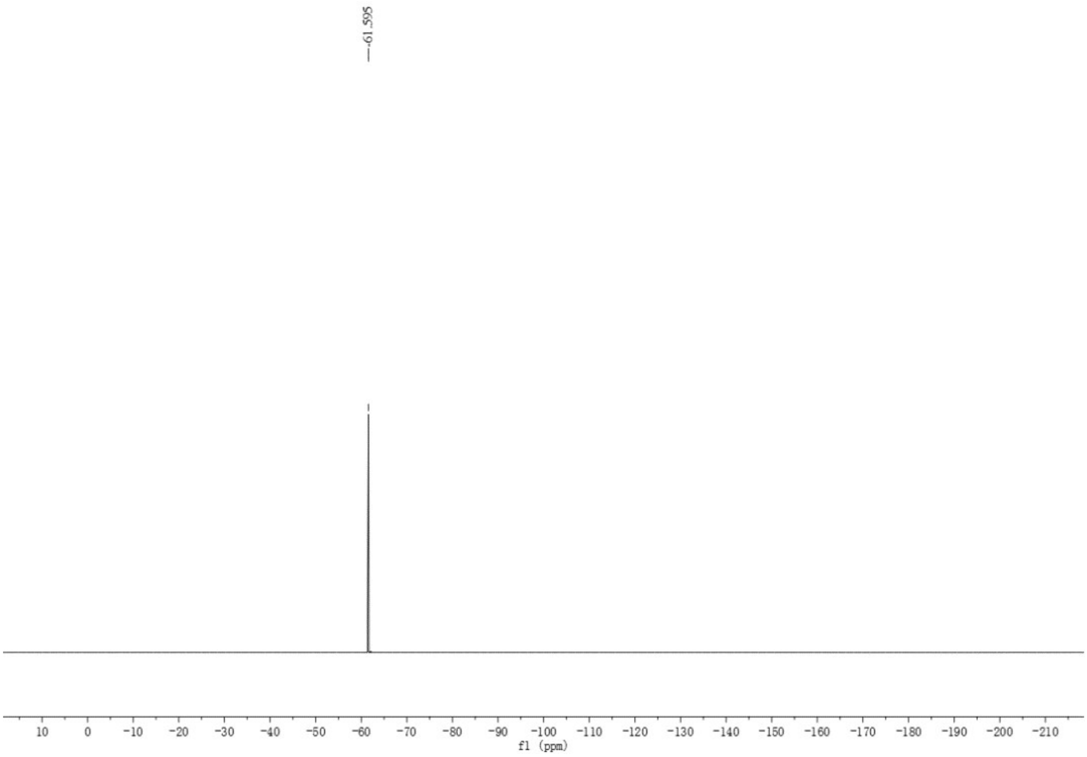

^{31}P NMR of $(cf_3bt)_2Ir(tpip)$

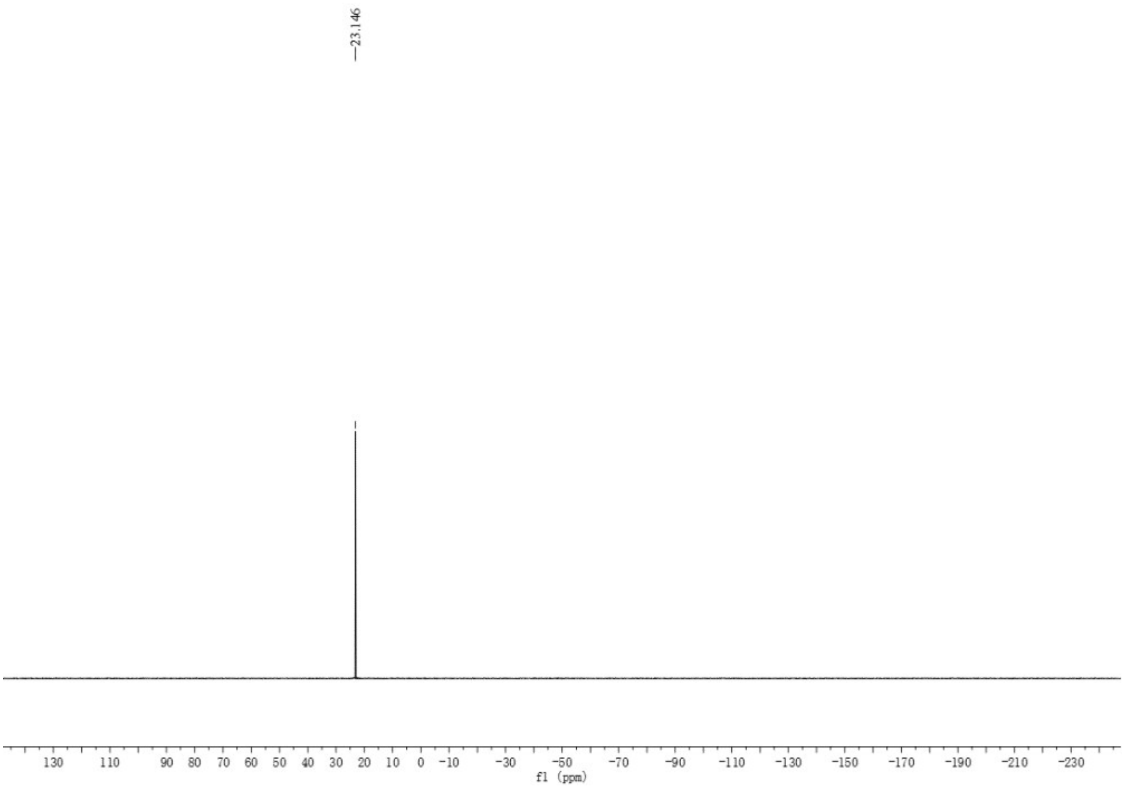

MS of $(dfbt)_2Ir(tpip)$

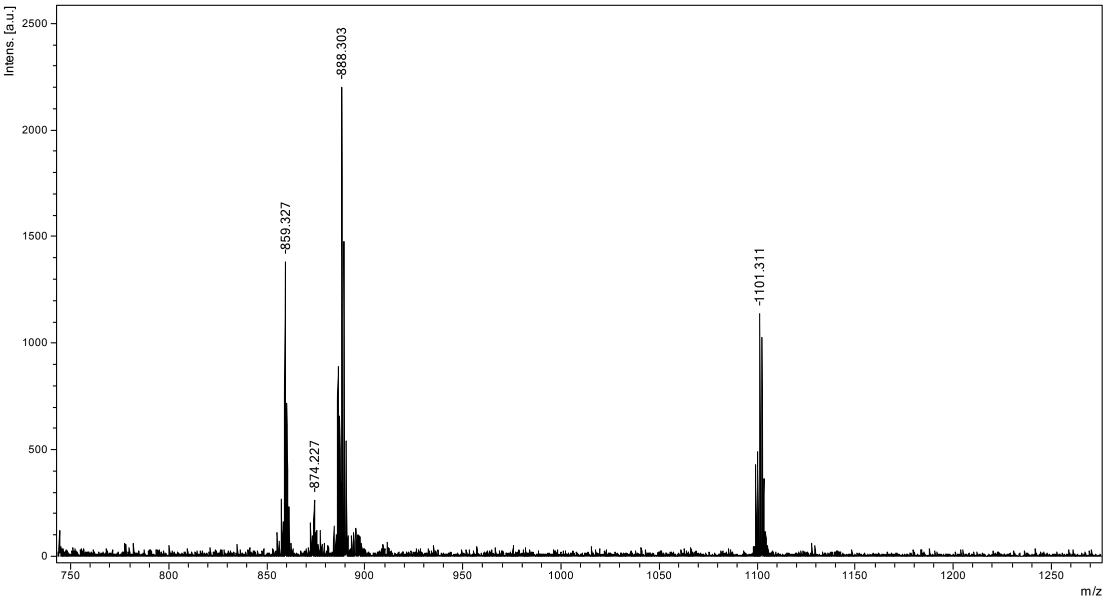

[1]H NMR of $(dfbt)_2Ir(tpip)$

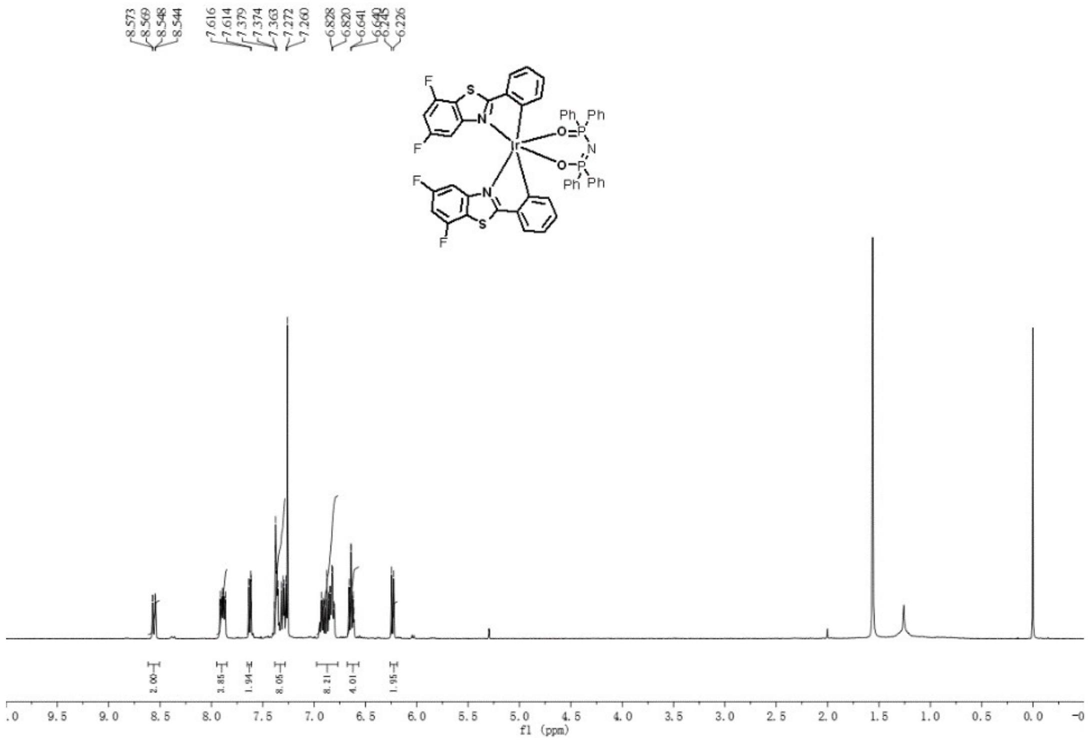

^{19}F NMR of $(dfbt)_2Ir(tpip)$

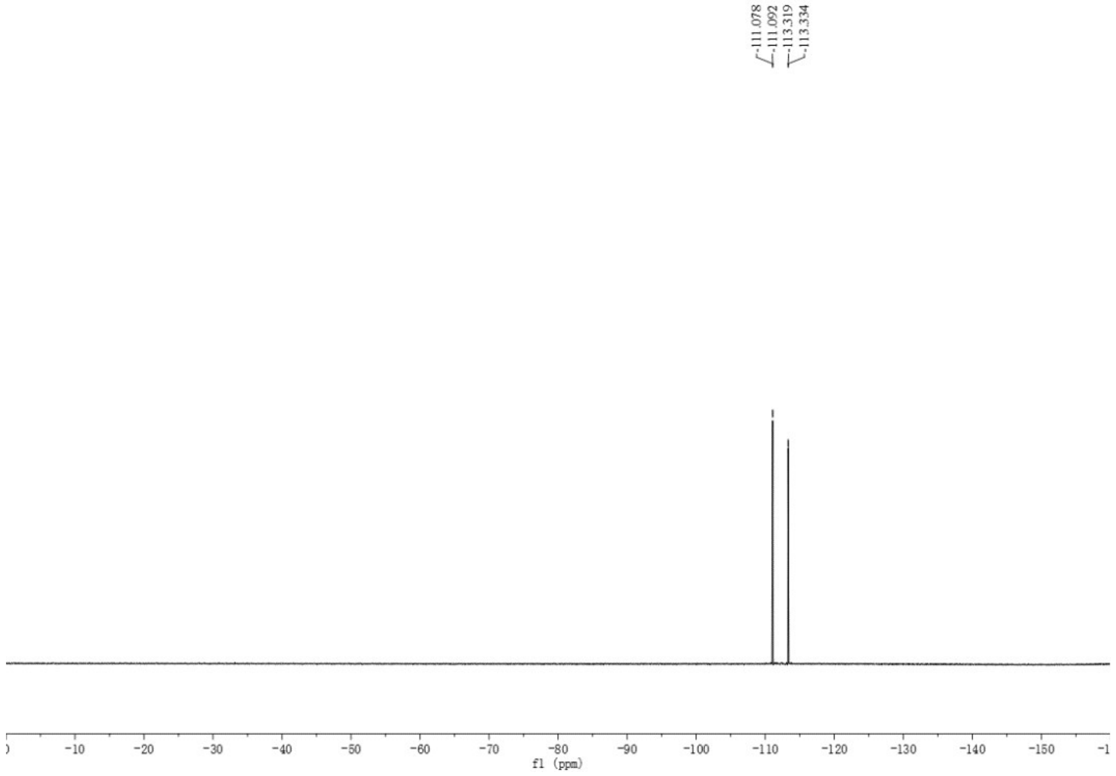

^{31}P NMR of $(dfbt)_2Ir(tpip)$

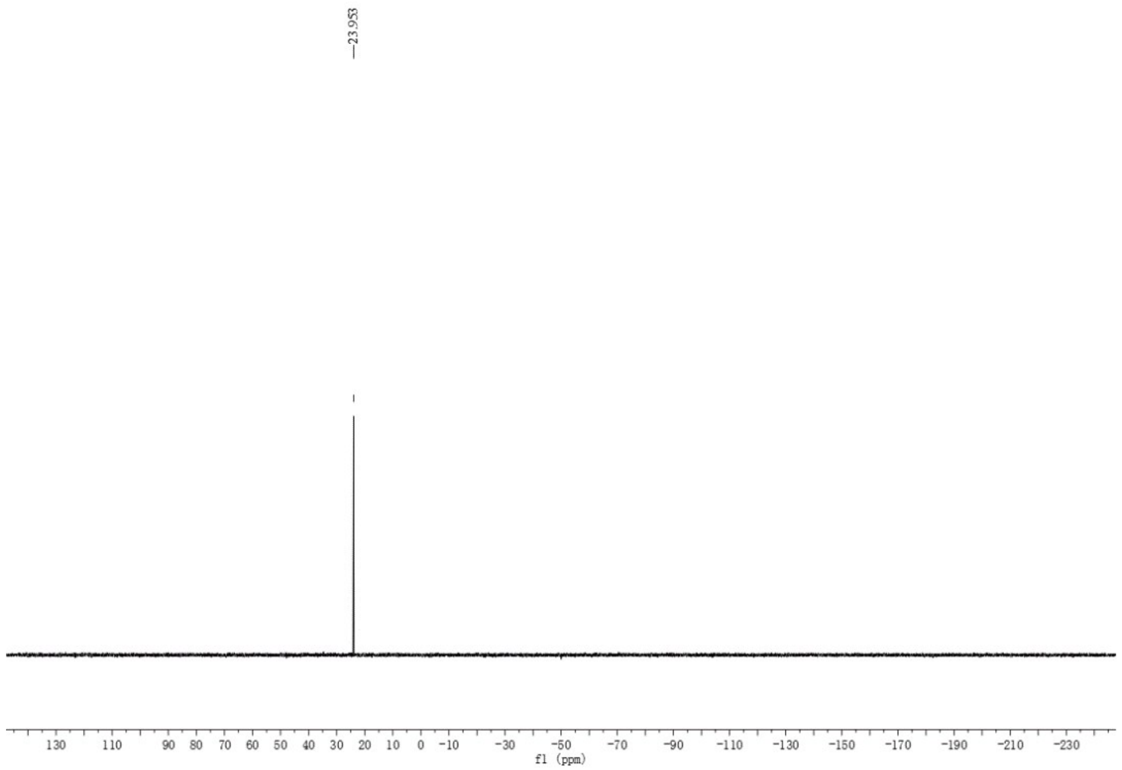

Table S1 Crystallographic data for complexes **$(bt)_2Ir(tpip)$**, **$(cf_3bt)_2Ir(tpip)$** and **$(dfbt)_2Ir(tpip)$**

	$(bt)_2Ir(tpip)$	**$(cf_3bt)_2Ir(tpip)$**	**$(dfbt)_2Ir(tpip)$**
Formula	$C_{50}H_{36}IrN_3O_2P_2S_2$	$C_{52}H_{34}F_6IrN_3O_2P_2S_2$	$C_{50}H_{29}F_4IrN_3O_2P_2S_2$
M_r	1029.08	1165.08	1098.02
Crystal system	Monoclinic	Triclinic	Orthorhombic
Space group	*C*2/c	$P\bar{1}$	$P2_12_12_1$
Wavelength / Å	0.7107	0.7107	0.7107
X-radiation (graphite monochromator)	Mo-Kα	Mo-Kα	Mo-Kα
T / K	293(2)	293(2)	293(2)
a (Å)	13.2664(3)	14.2112(3)	11.6332(3)
b (Å)	17.6254(4)	20.0703(5)	16.9857(6)
c (Å)	55.0222(17)	20.8334(4)	23.8858(8)
α (°)	90	109.056(2)	90
β (°)	93.977(2)	109.8998(18)	90
γ (°)	90	92.8019(18)	90
V (Å^3)	12834.6(6)	5194.9(2)	4719.8(3)
Z	12	4	4
ρ_c (gcm^{-3})	1.598	1.490	1.669
F(000)	6144	2304	2344
Absorption coefficient / mm^{-1}	3.338	2.775	3.043
index ranges	-18<=h<=13	-17<=h<=15	-10<=h<=14
	-24<=k<=17	-25<=k<=24	-21<=k<=19
	-69<=l<=70	-25<=l<=26	-23<=l<=29
GOF (F^2)	0.998	1.065	0.976
$R_1{}^a$,$wR_2{}^b$(I>2σ(I))	0.0673, 0.0923	0.0358, 0.0657	0.0395, 0.0608
$R_1{}^a$,$wR_2{}^b$(all data)	0.0875, 0.0991	0.0582, 0.0732	0.0582, 0.0668

$^aR_1 = \Sigma||F_o|-|F_c||/\Sigma|F_o|$. $^bwR_2 = [\Sigma w(F_o{}^2-F_c{}^2)^2/\Sigma w(F_o{}^2)]^{1/2}$

Table S2 Selected bond distances (Å) and angles (◦) for complexes **(bt)$_2$Ir(tpip)**, **(cf$_3$bt)$_2$Ir(tpip)** and **(dfbt)$_2$Ir(tpip)**

(bt)$_2$Ir(tpip)			
Ir(1)-O(1)	2.185(4)	Ir(1)-O(2)	2.210(4)
Ir(1)-N(1)	2.056(5)	Ir(1)-N(2)	2.056(5)
Ir(1)-C(1)	1.990(6)	Ir(1)-C(14)	1.987(6)
O(1)-Ir(1)-O(2)	89.98(15)	C(1)-Ir(1)-O(2)	87.9(2)
C(1)-Ir(1)-N(1)	80.6(2)	C(1)-Ir(1)-N(2)	95.3(2)
C(1)-Ir(1)-C(14)	95.8(2)	N(1)-Ir(1)-O(2)	88.59(18)
N(1)-Ir(1)-O(1)	96.53(19)	N(2)-Ir(1)-O(2)	97.16(18)
N(2)-Ir(1)-O(1)	87.82(18)	C(14)-Ir(1)-O(1)	86.5(2)
C(14)-Ir(1)-N(1)	93.7(2)	C(14)-Ir(1)-N(2)	80.8(2)
(cf$_3$bt)$_2$Ir(tpip)			
Ir(1)-O(1)	2.201(3)	Ir(1)-O(2)	2.259(2)
Ir(1)-N(1)	2.055(3)	Ir(1)-N(2)	2.064(3)
Ir(1)-C(13)	1.986(3)	Ir(1)-C(27)	1.980(4)
O(1)-Ir(1)-O(2)	89.08(9)	C(27)-Ir(1)-O(2)	92.52(12)
C(27)-Ir(1)-N(1)	93.91(13)	C(27)-Ir(1)-N(2)	80.26(14)
C(27)-Ir(1)-C(13)	90.80(14)	N(1)-Ir(1)-O(2)	99.55(10)
N(1)-Ir(1)-O(1)	87.32(10)	N(2)-Ir(1)-O(2)	86.54(10)
N(2)-Ir(1)-O(1)	98.33(11)	C(13)-Ir(1)-O(1)	87.59(12)
C(13)-Ir(1)-N(1)	80.29(13)	C(13)-Ir(1)-N(2)	93.96(13)
(dfbt)$_2$Ir(tpip)			
Ir(1)-O(2)	2.211(5)	Ir(1)-O(1)	2.207(5)
Ir(1)-C(13)	1.986(8)	Ir (1)-C(22)	1.991(8)
Ir(1)-N(1)	2.050(6)	Ir(1)-N(2)	2.056(6)
O(1)-Ir(1)-O(2)	90.46(19)	C(22)-Ir(1)-O(2)	89.7(3)
C(22)-Ir(1)-N(1)	93.8(3)	C(22)-Ir(1)-N(2)	80.8(3)
C(22)-Ir(1)-C(13)	93.7(3)	N(1)-Ir(1)-O(2)	95.5(2)
N(1)-Ir(1)-O(1)	88.3(2)	N(2)-Ir(1)-O(2)	91.1(2)

N(2)-Ir(1)-O(1)	97.1(2)	C(13)-Ir(1)-O(1)	86.3(3)
C(13)-Ir(1)-N(1)	80.7(3)	C(13)-Ir(1)-N(2)	93.0(3)

Table S3 Main experimental and calculated optical transitions for complexes **$(bt)_2Ir(tpip)$**, **$(fbt)_2Ir(tpip)$**, **$(cf_3bt)_2Ir(tpip)$** and **$(dfbt)_2Ir(tpip)$**

Complex	Orbital Excitations	Nature of Transition	Oscillation Strength	Calcd (nm)	Exptl (nm)
$(bt)_2Ir(tpip)$	HOMO → LUMO	$Ir(d\pi)/L_{bt}(\pi) \rightarrow L_{bt}(\pi^*)$	0.0957	455	486
$(fbt)_2Ir(tpip)$	HOMO → LUMO	$Ir(d\pi)/L_{fbt}(\pi) \rightarrow L_{fbt}(\pi^*)$	0.0970	454	484
$(cf_3bt)_2Ir(tpip)$	HOMO → LUMO	$Ir(d\pi)/L_{cf3bt}(\pi) \rightarrow L_{cf3bt}(\pi^*)$	0.1047	471	502
$(dfbt)_2Ir(tpip)$	HOMO → LUMO	$Ir(d\pi)/L_{dfbt}(\pi) \rightarrow L_{dfbt}(\pi^*)$	0.0989	467	504

Table S4 Frontier orbital energy and electron density distribution for complexes **$(bt)_2Ir(tpip)$**, **$(fbt)_2Ir(tpip)$**, **$(cf_3bt)_2Ir(tpip)$** and **$(dfbt)_2Ir(tpip)$**

Complex	Orbital	Energy (eV)	Ir	bt	tpip
$(bt)_2Ir(tpip)$	LUMO	-1.790	3.57	94.21	2.23
	HOMO	-5.273	51.76	43.55	4.69
$(fbt)_2Ir(tpip)$	LUMO	-1.819	3.76	93.82	2.42
	HOMO	-5.306	50.77	44.47	4.75
$(cf_3bt)_2Ir(tpip)$	LUMO	-2.039	3.63	94.36	2.01
	HOMO	-5.409	54.57	40.60	4.82
$(dfbt)_2Ir(tpip)$	LUMO	-2.006	3.40	94.52	2.09
	HOMO	-5.410	51.81	43.07	5.13

Table S5 Electrochemical and theoretical data of complexes **$(bt)_2Ir(tpip)$**, **$(fbt)_2Ir(tpip)$**, **$(cf_3bt)_2Ir(tpip)$** and **$(dfbt)_2Ir(tpip)$** (eV).

Complex	E_{ox}	HOMO/LUMO[a]	HOMO/LUMO[b]	$E_{opt,g}$[c]
$(bt)_2Ir(tpip)$	1.03	-5.83/-3.66	-5.27/-1.79	2.17
$(fbt)_2Ir(tpip)$	1.06	-5.86/-3.68	-5.31/-1.82	2.18
$(cf_3bt)_2Ir(tpip)$	1.15	-5.96/-3.80	-5.41/-2.04	2.14
$(dfbt)_2Ir(tpip)$	1.16	-5.95/-3.79	-5.41/-2.01	2.16

[a] Deduced from the equation HOMO = – (E_{ox} + 4.8 eV) and LUMO = HOMO + $E_{opt,g}$, respectively.

[b] Obtained from theoretical calculations. [c] Calculated from the UV-vis absorption edges.

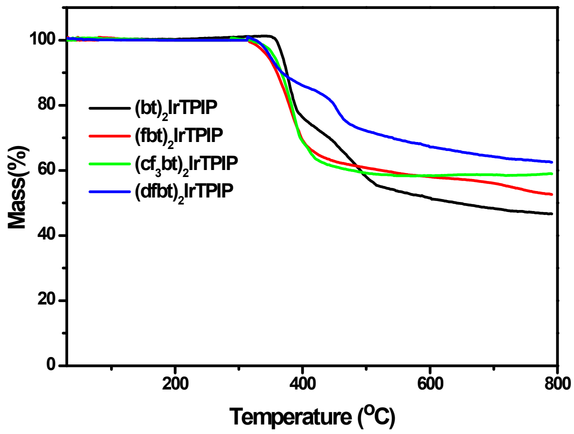

Fig. S1 TGA curves of complexes **(bt)$_2$Ir(tpip)**, **(fbt)$_2$Ir(tpip)**, **(cf$_3$bt)$_2$Ir(tpip)** and **(dfbt)$_2$Ir(tpip)**

Reference:

1. CrysAlisPro Version 1.171.36.21. Agilent Technologies Inc. Santa Clara, CA, USA, 2012.
2. L. Palatinus and G. Chapuis, *J. Appl. Crystallogr.,* 2007, **40**, 786.
3. G. M. Sheldrick, *Acta Crystallogr. Sect. A,* 2008, **64**, 112.
4. O. V. Dolomanov, L. J. Bourhis, R. J.Gildea, J. A. K. Howard and H. Puschmann, *J. Appl. Crystallogr.,* 2009, **42**, 339.
5. M. J. Frisch, G. W. Trucks, H. B. Schlegel, et al., Gaussian 09, Revision A.01, Gaussian, Wallingford, Con, USA, 2009.
6. C. Lee, W. Yang and R. G. Parr, *Phys. Rev. B.,* 1988, **37**, 785.
7. B. Miehlich, A. Savin, H. Stoll H. Preuss, *Chem. Phys. Lett.,* 1989, **157**, 200.
8. A. D. Becke, *J. Chem. Phys.*, 1993, **98**, 5648.